Acta Crystallographica Section B
Structural Science
ISSN 0108-7681

Structural comparisons of isomeric series of 7-aryl-benzo[*h*]pyrazolo[3,4-*b*]quinolines and 11-aryl-benzo[*f*]pyrazolo[3,4-*b*]quinolines

Jaime Portilla,[a] Jairo Quiroga,[a] Manuel Nogueras,[b] Jose M. de la Torre,[b] Justo Cobo,[b] John N. Low[c] and Christopher Glidewell[d]*

[a]Grupo de Investigación de Compuestos Heterocíclicos, Departamento de Química, Universidad de Valle, AA 25360 Cali, Colombia, [b]Departamento de Química Inorgánica y Orgánica, Universidad de Jaén, 23071 Jaén, Spain, [c]Department of Chemistry, University of Aberdeen, Meston Walk, Old Aberdeen AB24 3UE, Scotland, and [d]School of Chemistry, University of St Andrews, St Andrews, Fife KY16 9ST, Scotland

Correspondence e-mail: cg@st-andrews.ac.uk

Received 15 August 2007
Accepted 5 December 2007

The structures of three new 7-aryl-benzo[*h*]pyrazolo[3,4-*b*]-quinolines, 8-methyl-7-(4-chlorophenyl)-10-phenyl-6,10-dihydro-5*H*-benzo[*h*]pyrazolo[3,4-*b*]quinoline, $C_{27}H_{20}ClN_3$, 8-methyl-7-(3-pyridinyl)-10-phenyl-6,10-dihydro-5*H*-benzo[*b*]-pyrazolo[3,4-*b*]quinoline, $C_{26}H_{20}N_4$, and 8-methyl-7-(4-pyridinyl)-10-phenyl-10*H*-benzo[*h*]pyrazolo[3,4-*b*]quinoline, $C_{26}H_{18}N_4$, which is an unexpected oxidation product isolated from the attempted synthesis of 8-methyl-7-(4-pyridinyl)-10-phenyl-6,10-dihydro-5*H*-benzo[*h*]pyrazolo[3,4-*b*]quinoline, and those of three new 11-aryl-benzo[*f*]pyrazolo[3,4-*b*]quinolines, 11-(4-methylphenyl)-10-methyl-8-phenyl-6,8-dihydro-5*H*-benzo[*f*]pyrazolo[3,4-*b*]-quinoline, $C_{28}H_{23}N_3$ ($P\bar{1}$, $Z' = 2$), 11-(4-methoxyphenyl)-10-methyl-8-phenyl-6,8-dihydro-5*H*-benzo[*f*]pyrazolo[3,4-*b*]-quinoline, $C_{28}H_{23}N_3O$ ($P2_1/c$, $Z' = 4$), and 11-(3,4,5-trimethoxyphenyl)-10-methyl-8-phenyl-6,8-dihydro-5*H*-benzo-[*f*]pyrazolo[3,4-*b*]quinoline, $C_{30}H_{27}N_3O_3$, are reported. The crystal structures are compared with those of a number of analogues reported in the recent literature; in particular, structural comparisons are drawn within each series as the substituted pendent aryl group is varied, and between several pairs of strictly isomeric 7-aryl-benzo[*h*]pyrazolo[3,4-*b*]quinolines and 11-aryl-benzo[*f*]pyrazolo[3,4-*b*]quinolines containing the same aryl substituents within each pair. Intermolecular interactions of the C—H$\cdots\pi$ type are found in the crystal structures of both series, but $\pi\cdots\pi$ stacking interactions are found only in the 7-aryl-benzo[*h*]pyrazolo[3,4-*b*]quinoline series.

1. Introduction

Pyrazolo[3,4-*b*]quinolines are of interest because of their biological properties such as parasiticidic, bactericidal, vasodilator and enzyme-inhibitory activity, in addition to their potential as possible anti-viral and anti-malarial agents (Quiroga *et al.*, 2001). We have recently concentrated on the use of multicomponent cyclocondensation reactions, conducted using microwave irradiation under solvent-free conditions, for the synthesis of a range of fused heterocyclic systems containing the pyrazolo[3,4-*b*]quinoline unit. As part of this study, we have recently reported the molecular and crystal structures of a number of 7-aryl-8-methyl-10-phenyl-6,10-dihydro-5*H*-benzo[*h*]pyrazolo[3,4-*b*]quinolines, (I)–(III) (Portilla *et al.*, 2005*b*), and 11-aryl-10-methyl-8-phenyl-6,8-dihydro-5*H*-benzo[*f*]pyrazolo[3,4-*b*]quinolines, (X)–(XIII) (Portilla, Serrano *et al.*, 2005; Serrano *et al.*, 2005*a*,*b*). The two compound types contain sequences of four fused rings such that the two series, conveniently denoted *A* and *B*, respectively (see Scheme 1), have skeletons which are isomeric: in series *A* the fused aryl ring is on the edge of the molecule

opposite from the pendent aryl substituent, while in series *B* these rings are adjacent on the same edge.

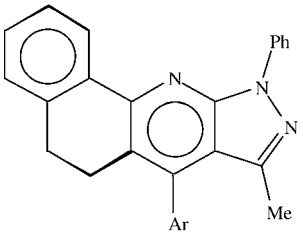

(A)

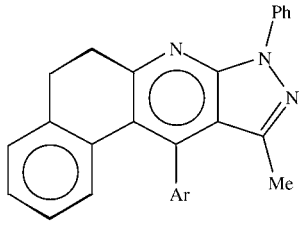

(B)

(I) Ar = C_6H_5
(II) Ar = 4-$CH_3C_6H_4$
(III) Ar = 4-$CH_3OC_6H_4$
(IV) Ar = 4-ClC_6H_4
(V) Ar = 3-pyridyl
(VI) Ar = 4-pyridyl

(VII) Ar = C_6H_5
(VIII) Ar = 4-$CH_3C_6H_4$
(IX) Ar = 4-$CH_3OC_6H_4$
(X) Ar = 4-ClC_6H_4
(XI) Ar = 3-pyridyl
(XII) Ar = 4-pyridyl
(XIII) Ar = 4-BrC_6H_4
(XIV) Ar = 3,4,5-$(MeO)_3C_6H_2$

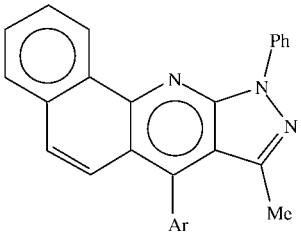

(XV) Ar = 4-pyridyl

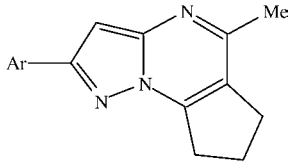

(XVI) Ar = 4-$CH_3C_6H_4$
(XVII) Ar = 4-ClC_6H_4
(XVIII) Ar = 4-BrC_6H_4

Scheme 1

Compounds in series *A* are readily and rapidly synthesized by microwave irradiation, in the absence of any solvent, of equimolar mixtures of 5-amino-3-methyl-1-phenylpyrazole and a substituted 2-methylene-1-tetralone, prepared separately by condensation of 1-tetralone and the corresponding aryl aldehyde (see Scheme 2). Compounds in series *B* are similarly prepared by microwave irradiation, using three-component mixtures, again in the absence of any solvent, containing 5-amino-3-methyl-1-phenylpyrazole, an aryl aldehyde and 2-tetralone. In each series the orientation of the terminal aryl ring of the fused ring system, relative to the pendent aryl group arising from the aldehyde component, is completely and reliably controlled by the location of the carbonyl group in the tetralone component. This carbonyl unit condenses with the amino group of the pyrazole component in the formation of the fused pyridine ring, and thereby controls the orientation of the terminal aryl ring.

In series *A*, (I) and (II) are both linked into sheets by two independent C—H$\cdots\pi$ hydrogen bonds, but C—H$\cdots$N hydrogen bonds are absent from both structures. While the two acceptors in (II) are two different aryl rings, in (I) the acceptor in one interaction is a pyridyl ring, and that in the other is an aryl ring, so the details of the sheet formation are different in (I) and (II). The hydrogen-bonded structure of (III), by contrast, is three-dimensional, and it exhibits C—H$\cdots$N and C—H$\cdots$O hydrogen bonds in addition to C—H$\cdots\pi$ interactions utilizing both pyridyl and aryl rings as the acceptors (Portilla *et al.*, 2005*b*). In contrast to the two- and three-dimensional structures observed to date in series *A*, the structures reported so far for members of series *B* all exhibit low-dimensional hydrogen-bonded structures. The isostructural pair (X) and (XIII) form chains of edge-fused rings built from two independent C—H$\cdots\pi$(arene) hydrogen bonds (Serrano *et al.*, 2005*a*,*b*), while the two isomeric pyridyl derivatives (XI) and (XII) respectively form cyclic tetramers built from a single C—H$\cdots$N hydrogen bond and isolated molecules (Portilla, Serrano *et al.*, 2005). Thus, the predominant forms of direction-specific intermolecular interactions in the examples of series *A* and *B* examined previously are C—H$\cdots\pi$ hydrogen bonds, with either aryl or pyridyl acceptors, with C—H$\cdots$N hydrogen bonds occurring rather less frequently: aromatic $\pi\cdots\pi$ stacking interactions have noticeably been absent.

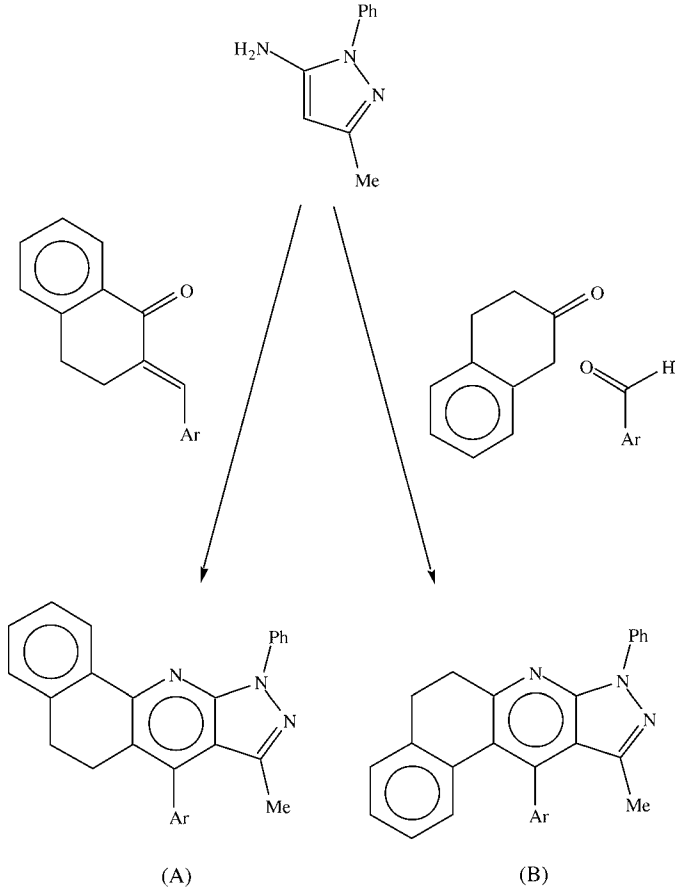

(A) (B)

Scheme 2

Continuing our study of the structural variations within these two series as the pendent aryl groups are varied systematically, we have now investigated a number of further examples in each series, taking the opportunity to compare a number of pairs of compounds, one from each series, having the identical aryl substituent, so that the two members of each pair are strictly isomeric. Thus, we report here on (IV) and (V)

Table 1
Experimental details.

	(IV)	(V)	(VIII)
Crystal data			
Chemical formula	$C_{27}H_{20}ClN_3$	$C_{26}H_{20}N_4$	$C_{28}H_{23}N_3$
M_r	421.91	388.46	401.49
Cell setting, space group	Monoclinic, $P2_1/c$	Monoclinic, $P2_1/c$	Triclinic, $P\bar{1}$
Temperature (K)	120 (2)	120 (2)	118 (2)
a, b, c (Å)	12.1072 (4), 14.2672 (5), 12.7635 (4)	11.2274 (6), 13.7079 (8), 12.6935 (7)	11.1334 (3), 11.4672 (2), 17.6270 (4)
α, β, γ (°)	90.00, 109.953 (8), 90.00	90.00, 95.731 (3), 90.00	97.858 (2), 106.135 (3), 97.496 (2)
V (Å^3)	2072.37 (16)	1943.82 (19)	2107.66 (9)
Z	4	4	4
D_x (Mg m^{-3})	1.352	1.327	1.265
Radiation type	Mo $K\alpha$	Mo $K\alpha$	Mo $K\alpha$
μ (mm^{-1})	0.21	0.08	0.08
Crystal form, colour	Lath, colourless	Plate, colourless	Block, colourless
Crystal size (mm)	0.38 × 0.38 × 0.10	0.12 × 0.10 × 0.02	0.20 × 0.18 × 0.12
Data collection			
Diffractometer	Bruker–Nonius KappaCCD	Bruker–Nonius KappaCCD	Bruker–Nonius KappaCCD
Data collection method	φ and ω scans	φ and ω scans	φ and ω scans
Absorption correction	Multi-scan	Multi-scan	Multi-scan
T_{min}	0.936	0.987	0.982
T_{max}	0.980	0.998	0.991
No. of measured, independent and observed reflections	23 840, 4752, 3209	19 684, 4456, 2654	40 500, 9647, 7878
Criterion for observed reflections	$I > 2\sigma(I)$	$I > 2\sigma(I)$	$I > 2\sigma(I)$
R_{int}	0.052	0.085	0.048
θ_{max} (°)	27.5	27.5	27.5
Refinement			
Refinement on	F^2	F^2	F^2
$R[F^2 > 2\sigma(F^2)]$, $wR(F^2)$, S	0.051, 0.130, 1.02	0.068, 0.137, 1.03	0.044, 0.108, 1.03
No. of reflections	4752	4456	9647
No. of parameters	281	272	564
H-atom treatment	Constrained to parent site	Constrained to parent site	Constrained to parent site
Weighting scheme	$w = 1/[\sigma^2(F_o^2) + (0.0643P)^2 + 0.6125P]$, where $P = (F_o^2 + 2F_c^2)/3$	$w = 1/[\sigma^2(F_o^2) + (0.0367P)^2 + 0.9505P]$, where $P = (F_o^2 + 2F_c^2)/3$	$w = 1/[\sigma^2(F_o^2) + (0.0391P)^2 + 0.8878P]$, where $P = (F_o^2 + 2F_c^2)/3$
$(\Delta/\sigma)_{max}$	0.001	< 0.0001	< 0.0001
$\Delta\rho_{max}$, $\Delta\rho_{min}$ (e Å^{-3})	0.58, −0.43	0.23, −0.21	0.27, −0.25
Extinction method	None	None	*SHELXL*
Extinction coefficient	–	–	0.0084 (11)

	(IX)	(XIV)	(XV)
Crystal data			
Chemical formula	$C_{28}H_{23}N_3O$	$C_{30}H_{27}N_3O_3$	$C_{26}H_{18}N_4$
M_r	417.49	477.55	386.44
Cell setting, space group	Monoclinic, $P2_1/c$	Monoclinic, Cc	Monoclinic, $P2_1/c$
Temperature (K)	120 (2)	120 (2)	120 (2)
a, b, c (Å)	18.0854 (3), 21.2296 (5), 23.8007 (5)	10.4716 (9), 20.0027 (18), 12.1529 (9)	11.3560 (3), 17.3507 (5), 9.7577 (2)
β (°)	108.2580 (10)	107.818 (4)	97.262 (2)
V (Å^3)	8678.1 (3)	2423.4 (4)	1907.18 (8)
Z	16	4	4
D_x (Mg m^{-3})	1.278	1.309	1.346
Radiation type	Mo $K\alpha$	Mo $K\alpha$	Mo $K\alpha$
μ (mm^{-1})	0.08	0.09	0.08
Crystal form, colour	Lath, colourless	Plate, colourless	Lath, colourless
Crystal size (mm)	0.90 × 0.30 × 0.10	0.60 × 0.30 × 0.02	0.50 × 0.24 × 0.10
Data collection			
Diffractometer	Bruker–Nonius KappaCCD	Bruker–Nonius KappaCCD	Bruker–Nonius KappaCCD
Data collection method	φ and ω scans	φ and ω scans	φ and ω scans
Absorption correction	Multi-scan	Multi-scan	Multi-scan
T_{min}	0.934	0.963	0.971
T_{max}	0.992	0.998	0.992
No. of measured, independent and observed reflections	99 695, 19 715, 8289	20 344, 2720, 1499	26 391, 4372, 2818
Criterion for observed reflections	$I > 2\sigma(I)$	$I > 2\sigma(I)$	$I > 2\sigma(I)$
R_{int}	0.166	0.199	0.064
θ_{max} (°)	27.5	27.5	27.5

Table 1 (continued)

	(IX)	(XIV)	(XV)
Refinement			
Refinement on	F^2	F^2	F^2
$R[F^2 > 2\sigma(F^2)]$, $wR(F^2)$, S	0.096, 0.169, 0.98	0.055, 0.152, 1.08	0.050, 0.142, 1.01
No. of reflections	19 715	2720	4372
No. of parameters	1161	329	272
H-atom treatment	Constrained to parent site	Constrained to parent site	Constrained to parent site
Weighting scheme	$w = 1/[\sigma^2(F_o^2) + (0.0682P)^2]$, where $P = (F_o^2 + 2F_c^2)/3$	$w = 1/[\sigma^2(F_o^2) + (0.0625P)^2]$, where $P = (F_o^2 + 2F_c^2)/3$	$w = 1/[\sigma^2(F_o^2) + (0.0831P)^2]$, where $P = (F_o^2 + 2F_c^2)/3$
$(\Delta/\sigma)_{max}$	< 0.0001	< 0.0001	< 0.0001
$\Delta\rho_{max}$, $\Delta\rho_{min}$ (e Å^{-3})	0.26, −0.30	0.45, −0.55	0.33, −0.34
Extinction method	None	None	None
Absolute structure	–	Friedel pairs merged	–

in series *A*, together with (XV) which was unexpectedly obtained from the attempted crystallization of (VI), and on (VIII), (IX) and (XIV) in series *B*. These results enable a more general comparison of the molecular and crystal structures across the entire series *A* and *B*. This study has revealed some unexpected variations in the crystallization characteristics, as well as in the details of the supramolecular aggregations.

2. Experimental

2.1. Syntheses

For the synthesis of compounds in series *A*, equimolar quantities (1 mmol of each component) of 5-amino-3-methyl-1-phenylpyrazole and a substituted 2-methylene-1-tetralone derived from 1-tetralone and the corresponding aldehyde, 4-chlorobenzaldehyde for (IV) and a pyridinecarboxaldehyde for (V) and (VI), were placed in open Pyrex vessels and irradiated in a domestic microwave oven for 3–5 min at 600 W. The product mixtures were extracted with ethanol and, after removal of the solvent, the products were recrystallized from dimethylformamide to give crystals of (IV) and (V) suitable for single-crystal X-ray diffraction. (IV) yellow crystals, 78% yield, m.p. 468–469 K, MS (30 eV) *m*/*z* (%) 423/421 (34/100, M^+), 408/406 (3/4), HRMS *m*/*z* found 421.1342, $C_{27}H_{20}{}^{35}ClN_3$ requires 421.1346. (V) yellow crystals, 54% yield, m.p. 558–559 K, MS (30 eV) *m*/*z* (%) 388 (100, M^+), 373 (5), HRMS *m*/*z* found 388.1685, $C_{26}H_{20}N_4$ requires 388.1688. Compound (VI) was similarly prepared, 62% yield, m.p. 474–471 K, MS (30 eV) *m*/*z* (%) 388 (100, M^+), 373 (9), but it was found to be contaminated with a small quantity of (XV) which proved to be the only component providing satisfactory crystals: HRMS *m*/*z* found 386.1532, $C_{26}H_{18}N_4$ requires 386.1531. For the synthesis of compounds in series *B*, equimolar quantities (1 mmol of each component) of 5-amino-3-methyl-1-phenylpyrazole, 2-tetralone and a substituted benzaldehyde, 4-tolualdehyde for (VIII), 4-methoxybenzaldehyde for (IX) and 3,4,5-trimethoxybenzaldehyde for (XIV), were placed in open Pyrex vessels and irradiated in a domestic microwave oven for 3–5 min at 600 W. The product mixtures were extracted with ethanol and, after removal of the solvent, the products (VIII), (IX) and (XIV) were recrystallized from dimethylformamide to give crystals suitable for single-crystal X-ray diffraction. (VIII) yellow crystals, 70% yield, m.p. 478–479 K, MS (30 eV) *m*/*z* (%), 401 (100, M^+), 386 (10), HRMS *m*/*z* found 401.1891, $C_{28}H_{23}N_4$ requires 401.1891. (IX) yellow crystals, 75% yield, m.p. 430–431 K, MS (70 eV) *m*/*z* (%) 417 (100, M^+), 402 (7), HRMS *m*/*z* found 417.1829, $C_{28}H_{23}N_3O$ requires 417.1841. (XIV) yellow crystals, 70% yield, m.p. 421–422 K, MS (30 eV) *m*/*z* (%) 477 (100, M^+), 462 (8), HRMS *m*/*z* found 477.2055, $C_{30}H_{27}N_3O_3$ requires 477.2052.

2.2. Data collection, structure solution and refinement

Diffraction data for (IV), (V), (VIII), (IX), (XIV) and (XV) were collected at 120 (2) K using a Nonius Kappa CCD diffractometer: in all these cases graphite-monochromated Mo $K\alpha$ radiation (λ = 0.71073 Å) was employed. Other details of cell data, data collection and refinement are summarized in Table 1, together with details of the software employed (Burla *et al.*, 2005; Ferguson, 1999; Hooft, 1999; McArdle, 2003; Otwinowski & Minor, 1997; Sheldrick, 2003, 2008; Spek, 2003). For each of (IV), (V), (IX) and (XV), the space group $P2_1/c$ was uniquely assigned from the systematic absences. Crystals of (VIII) are triclinic, and the space group $P\bar{1}$ was selected and subsequently confirmed by the successful structure analysis. For (XIV) the systematic absences permitted $C2/c$ and Cc as possible space groups: Cc was selected and confirmed by the subsequent structure analysis. The structures were solved by direct methods and refined against all data on F^2. A weighting scheme based upon $P = [F_o^2 + 2F_c^2]/3$ was employed in order to reduce statistical bias (Wilson, 1976). All H atoms were located from difference maps and then treated as riding atoms with C—H distances of 0.95 Å (aryl, heteroaryl or alkenyl), 0.98 Å (methyl) or 0.99 Å (methylene), and with U_{iso}(H) = $1.2U_{eq}$(C) or $1.5U_{eq}$(C) for the methyl groups. In the absence of significant resonant scattering the correct orientation of the structure of (XIV) with respect to the polar axis directions could not be established, and hence the Friedel equivalent reflections were merged prior to the final refinements. The crystal quality for both (IX) and (XIV) was poor and the crystals were fragile, such that attempts to cut small fragments from larger crystals consistently led to shattering of the crys-

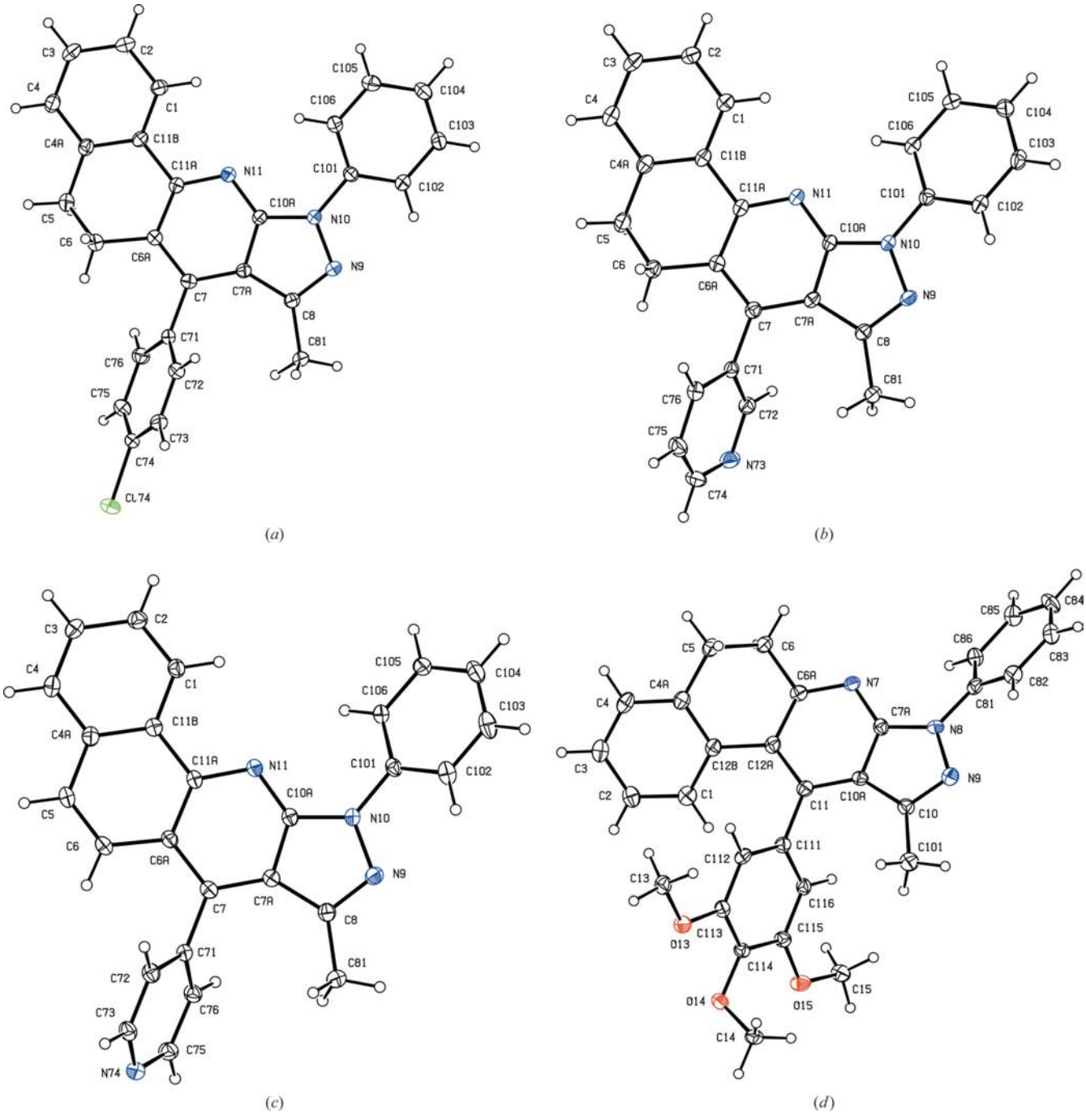

Figure 1
Molecules of (*a*) compound (IV), (*b*) compound (V), (*c*) compound (XV) and (*d*) compound (XIV) showing the atom-labelling schemes. Displacement ellipsoids are drawn at the 30% probability level.

tals: hence for these two compounds, the crystals used for the data collections were somewhat larger than is conventional. In addition, the poor crystal quality was manifested in the rather large merging indices and, for (IX), by the low proportion, just over 42%, of the data labelled observed, even at 120 K. Compound (IX) crystallizes with $Z' = 4$, but the ADDSYM routine in *PLATON* (Spek, 2003) gave no indication either of additional symmetry or of an alternative unit cell: this conclusion was confirmed by detailed scrutiny of the atom coordinates. No evidence for any form of twinning was found in any of the compounds reported here. Supramolecular analyses were made and the diagrams were prepared with the aid of *PLATON* (Spek, 2003). Details of molecular conformations are given in Table 2, and details of hydrogen-bond dimensions are given in Table 3.[1] Figs. 1–3 show the molecular

[1] Supplementary data for this paper are available from the IUCr electronic archives (Reference: BM5050). Services for accessing these data are described at the back of the journal.

Table 2
Ring-puckering angles and selected dihedral angles (°).

Angle α denotes the dihedral angle between the pyrazole ring and its pendent aryl ring; β denotes the dihedral angle between the pyridine ring and its pendent aryl ring.

	θ	φ	α	β
Series *A*				
(IV)†	119.0 (3)	36.2 (3)	20.9 (2)	63.7 (2)
(V)†	118.4 (2)	28.4 (4)	24.4 (2)	61.2 (2)
(XV)	–	–	32.2 (2)	64.4 (2)
Series B				
(VIII)‡				
Molecule 1	108.6 (2)	27.8 (2)	24.3 (2)	58.7 (2)
Molecule 2	106.5 (2)	28.6 (2)	14.2 (2)	57.1 (2)
(IX)‡				
Molecule 1	109.2 (3)	25.7 (3)	27.5 (2)	64.6 (2)
Molecule 2	109.2 (3)	29.1 (3)	15.5 (2)	61.6 (2)
Molecule 3	109.0 (3)	27.6 (3)	6.8 (2)	65.1 (2)
Molecule 4	109.5 (3)	27.3 (3)	7.8 (2)	67.8 (2)
(XIV)§	108.3 (7)	30.1 (7)	42.1 (3)	63.2 (3)

† Ring-puckering angles for the atom sequence (C11*A*,C11*B*,C4*A*,C5,C6,C6*A*). ‡ Ring-puckering angles for the atom sequences (C*x*2*A*,C*x*2*B*,C*x*4*A*,C*x*5,C*x*6,C*x*6*A*), where *x* = 1 or 2 in (VIII) and 1–4 in (IX). § Ring-puckering angles for the atom sequence (C12*A*,C12*B*,C4*A*,C5,C6,C6*A*).

components, with the atom-labelling schemes, and Figs. 4–7 show aspects of the crystal structures.

3. Results and discussion

3.1. Crystallization characteristics

In series *A* compounds (IV), (V) and (XV) (Fig. 1) all crystallize in the space group $P2_1/c$, with $Z' = 1$, as do (I)–(III) (Portilla *et al.*, 2005*b*). The 4-chlorophenyl compound (IV) is isomorphous and isostructural with the 4-methylphenyl compound (II). In addition, (XV) has unit-cell dimensions and atomic coordinates which are similar to those of (I); these two compounds are isomorphous, but not strictly isostructural since (XV) exhibits C—H···N hydrogen bonds with the pendent pyridyl providing the acceptor, whereas (I) cannot form such hydrogen bonds. On the other hand, there is no obvious resemblance between the unit-cell dimensions of (V) and those of (I).

By contrast with the common space group and Z' value found throughout series *A*, the members of series *B* (Figs. 1–3) all crystallize with different combinations of space group and Z' values. Thus, the 4-methylphenyl derivative (VIII) has $Z' = 2$ in the space group $P\bar{1}$; the 4-methoxyphenyl compound (IX) has $Z' = 4$ in the space group $P2_1/c$; the 4-chlorophenyl compound (X) has $Z' = 1$ in the space group $P\bar{1}$, as has the isostructural 4-bromophenyl analogue (XIII) (Serrano *et al.*, 2005*a*,*b*); and the 3-pyridyl derivative (XI) has $Z' = 1$ in space group $P\bar{4}2_1c$ (Portilla, Serrano *et al.*, 2005). In addition, the 4-pyridyl compound (XII) which is closely related to (XV) differs from it by crystallizing in the space group $P2_12_12$ with $Z' = 2$ (Portilla, Serrano *et al.*, 2005).

However, there are no resemblances whatsoever between the unit-cell dimensions or space groups within the pairs of isomers (II) and (VIII), (III) and (IX), (IV) and (X), (V) and (XI), or between those of (XV) and (XII). Thus, whereas in series *A* the 4-chlorophenyl and 4-methylphenyl derivatives are isostructural, as often found in such pairs, in series *B* they are not isostructural although the 4-chlorophenyl and 4-bromophenyl derivatives are isostructural (Serrano *et al.*, 2005*a*,*b*): we may note in this connection that the series of compounds (XVI)–(XVIII) are all isostructural (Portilla *et al.*, 2005*a*).

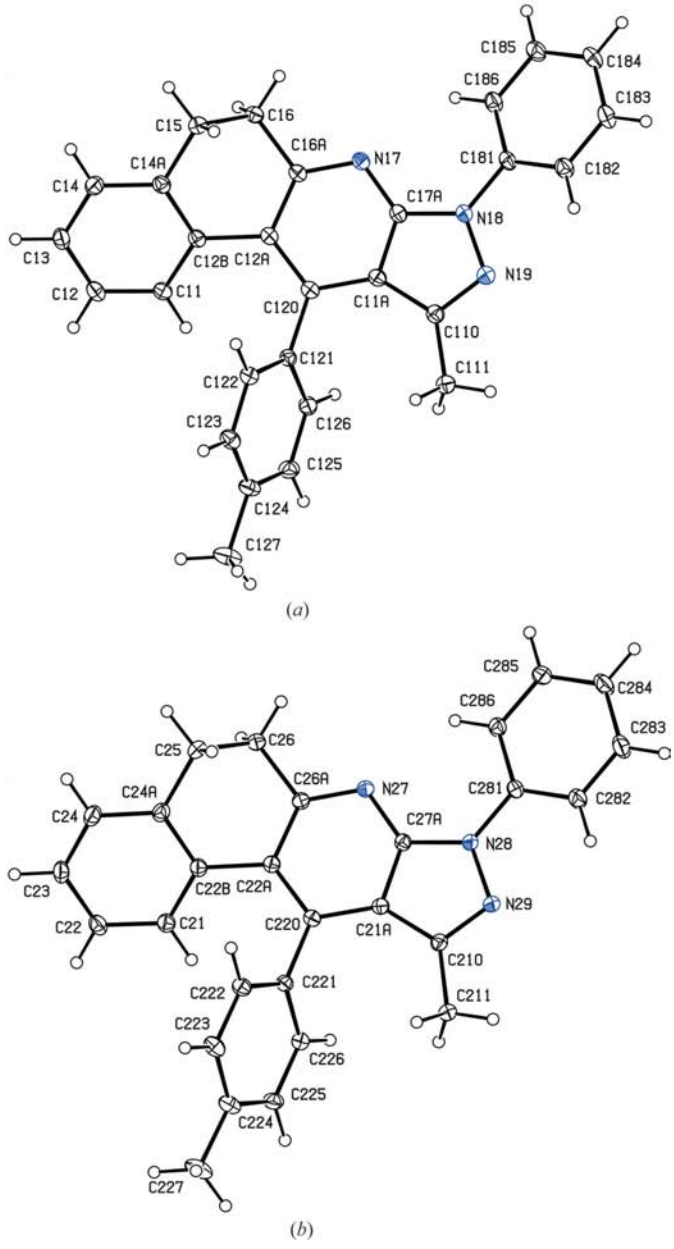

Figure 2
The two independent molecules of (VIII) showing the atom-labelling scheme. Displacement ellipsoids are drawn at the 30% probability level.

3.2. Molecular dimensions and conformations

For both series *A* and *B*, the bond lengths within the fused heterocyclic systems indicate clearly that there is electronic

delocalization within the pyridyl portion accompanied by significant bond fixation within the pyrazole portion: the bond lengths also clearly reflect the double-bond character of C5—C6 in (XV), as opposed to the single-bond character of the equivalent bond in all of the other compounds discussed here.

In each of (IV), (V), (VIII), (IX) and (XIV) the ring-puckering parameters (Cremer & Pople, 1975) indicate (Table 2) that the non-aromatic carbocyclic ring adopts a conformation best described as screw boat, for which the idealized parameters are $\theta = 112.5^\circ$ and $\varphi = (60n + 30)^\circ$, where n is zero or an integer. Similar conformations have also been observed in (I)–(III) (Portilla *et al.*, 2005*b*), (X) (Serrano *et al.*, 2005*a*), (XI) and (XII) (Portilla, Serrano *et al.*, 2005) and (XIII) (Serrano *et al.*, 2005*b*). Accordingly, the molecules in (IV), (V), (VIII), (IX) and (XIV) all lack any internal symmetry and hence they are chiral, although in every case the space group accommodates equal numbers of the two enantiomeric forms. The asymmetric units have been selected in all of the

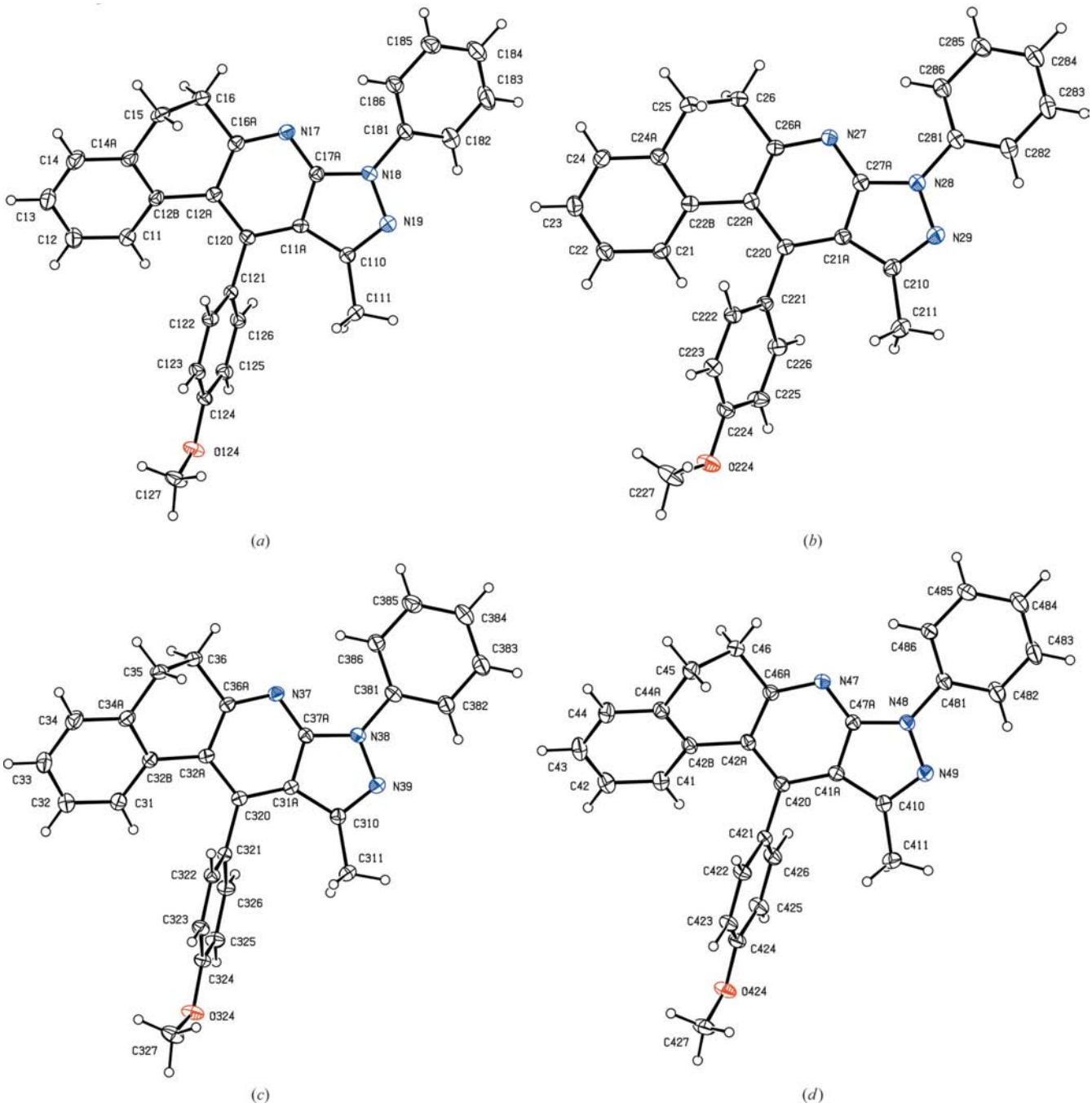

Figure 3
The four independent molecules of (IX) showing the atom-labelling scheme. Displacement ellipsoids are drawn at the 30% probability level.

Table 3
Hydrogen-bond parameters (Å, °).

	D—H···A	H···A	D···A	D—H···A
Series *A*				
(IV)	C72—H72···Cg1^{i,a}	2.88	3.823 (2)	170
	C75—H75···Cg2^{ii,b}	2.94	3.860 (2)	164
(V)	C72—H72···Cg1^{i,a}	2.79	3.706 (3)	163
	C75—H75···Cg2^{iii,b}	2.66	3.431 (3)	139
(XV)	C72—H72···N11^{iv}	2.56	3.404 (2)	149
	C4—H4···Cg3^{i,c}	2.84	3.771 (2)	165
	C4—H4···Cg4^{i,d}	2.92	3.700 (2)	140
	C75—H75···Cg2^{v,b}	2.60	3.463 (2)	151
	C103—H103···Cg5^{vi,e}	2.87	3.749 (2)	154
Series *B*				
(VIII)	C21—H2···Cg6^{vii,f}	2.89	3.662 (2)	136
	C122—H122···Cg7^{g}	2.75	3.412 (2)	127
	C125—H125···Cg8^{iv,h}	2.87	3.772 (2)	160
	C222—H222···Cg9^{j}	2.75	3.322 (2)	119
	C225—H225···Cg10^{viii,k}	2.93	3.834 (2)	160
(IX)	C24—H24···N39	2.60	3.504 (3)	159
	C326—H326···N47	2.59	3.526 (3)	168
	C122—H122···Cg11*m*	2.77	3.542 (3)	139
	C222—H222···Cg12^{ix,n}	2.77	3.568 (3)	142
	C225—H225···Cg8^{x,h}	2.76	3.628 (3)	152
	C322—H322···Cg7$_{xi,g}$	2.77	3.483 (3)	132
	C422—H422···Cg9^{j}	2.83	3.693 (3)	152
(XIV)	C82—H82···Cg13^{xii,p}	2.73	3.472 (6)	130

Symmetry codes: (i) $x, \frac{1}{2}-y, \frac{1}{2}+z$; (ii) $-x, \frac{1}{2}+y, \frac{1}{2}-z$; (iii) $1-x, \frac{1}{2}+y, \frac{3}{2}-z$; (iv) $1-x, 1-y, 1-z$; (v) $1-x, 1-y, -z$; (vi) $1-x, \frac{1}{2}+y, \frac{1}{2}-z$; (vii) $1-x, 1-y, 2-z$; (viii) $-1+x, y, z$; (ix) $1-x, -\frac{1}{2}+y, \frac{1}{2}-z$; (x) $2-x, -\frac{1}{2}+y, \frac{1}{2}-z$; (xi) $1-x, \frac{1}{2}+y, \frac{1}{2}-z$; (xii) $x, 1-y, -\frac{1}{2}+z$. (*a*) Cg1 is the centroid of ring (C1,C2,C3,C4,C4*A*,C11*B*); (*b*) Cg2 is the centroid of ring (C101–C106); (*c*) Cg3 is the centroid of ring (N11,C10*A*,C7*A*,C7,C6*A*,C11*A*); (*d*) Cg4 is the centroid of ring (C4*A*,C5,C6,C6*A*,C11*A*,C11*B*); (*e*) Cg5 is the centroid of ring (C71,C72,C73,N74,C75,C76); (*f*) Cg6 is the centroid of ring (C281–C286); (*g*) Cg7 is the centroid of ring (N27,C26*A*,C22*A*,C220,C21*A*,C27*A*); (*h*) Cg8 is the centroid of ring (C181–C186); (*j*) Cg9 is the centroid of ring (N17,C16*A*,C12*A*,C120,C11*A*,C17*A*); (*k*) Cg10 is the centroid of ring (C121–C126); (*m*) Cg11 is the centroid of ring (N47,C46*A*,C42*A*,C420,C41*A*,C47*A*); (*n*) Cg12 is the centroid of ring (N37,C36*A*,C32*A*,C320,C31*A*,C37*A*); (*p*) Cg13 is the centroid of ring (N7,C6*A*,C11*A*,C11,C10*A*,C7*A*).

compounds reported here to contain non-aromatic carbocyclic rings of the same hand. In addition, the asymmetric units in (VIII) and (IX) were selected so that the independent molecules were connected by hydrogen bonds within the asymmetric units.

The aryl substituents pendent from the pyridyl rings are twisted out of the plane of the fused heterocyclic system to a much greater extent than the aryl substituents pendent from the pyrazole rings, probably because of the more extensive non-bonded intramolecular H···H repulsions involving the pyridyl substituent.

3.3. Crystal structures

The supramolecular aggregation is dominated by hydrogen bonds of both C—H···N and C—H···π types (Table 3) and, in the case of series *A*, by $\pi\cdots\pi$ stacking interactions: the latter, however, are absent from the structures in series *B*. Of the short intermolecular contacts indicated by *PLATON* (Spek, 2003) as possible hydrogen bonds we have rejected all of those involving methyl C—H bonds as the potential donors. Not only are methyl C—H bonds expected to be of rather low acidity but, in general, methyl groups CH_3-E undergo extremely fast rotation about the C—E bonds even in the solid state, as shown by solid-state NMR spectroscopy (Riddell & Rogerson, 1996, 1997). In addition, it is well known (Tannenbaum *et al.*, 1956; Naylor & Wilson, 1957) that sixfold rotational barriers to intramolecular rotation are extremely low: barriers of this type are encountered when a fragment of local C_3 symmetry (such as methyl or *tert*-butyl) is bonded to a fragment with effective local C_2 symmetry (such as a planar ring) and the heights of these barriers are typically a few tens of J mol^{-1}. Contacts of the type C—H···π occur in (VIII), (IX) and (XIV), while similar contacts of C—H···O and C—H···N types occur in (XIV). From a collation of the results of a number of high-level *ab initio* investigations of various types of C—H···π interaction, it was concluded (Nishio, 2004) that those involving C—H bonds from methyl groups formed the weakest interactions This and the fast rotation of the methyl groups about the C—E bonds renders such contacts in this series structurally insignificant.

3.3.1. Series A. *Compound (IV)*: Compound (IV) (Fig. 1*a*) is isostructural with (II) (Portilla *et al.*, 2005*a*), with the molecules linked by two independent C—H···π(arene) hydrogen bonds into sheets parallel to (100). The sheet contains a single $\pi\cdots\pi$ stacking interaction. The pyridyl ring of the molecule at (x, y, z) and the aryl ring (C1, C2, C3, C4, C4*A*, C11*B*) of the molecule at ($-x, 1-y, -z$), which lie in

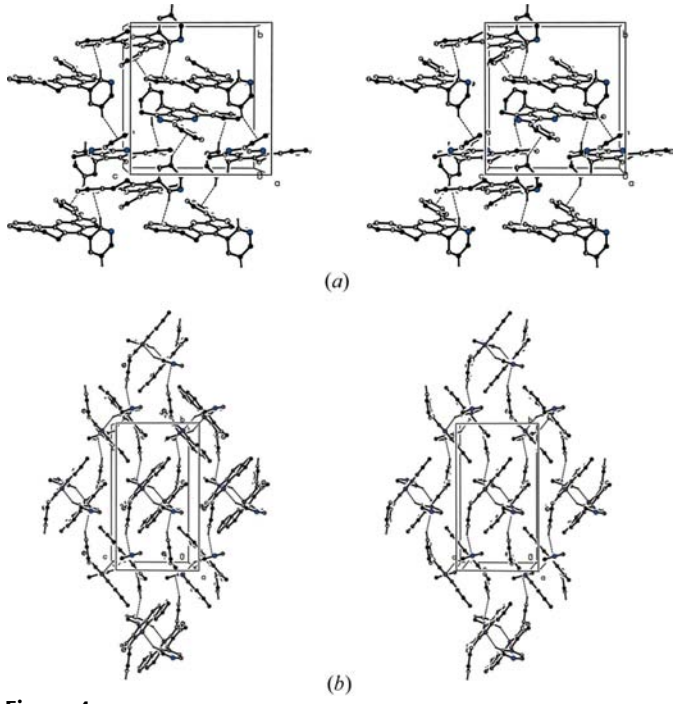

Figure 4
Stereoview of parts of the crystal structure of (V) and (XV) showing (*a*) the sheet parallel to (100) in (V) built from two C—H···π(arene) hydrogen bonds, and (*b*) the sheet parallel to (100) in (XV) built from C—H···N and C—H···π(pyridyl) hydrogen bonds. For the sake of clarity, the H atoms not involved in the motifs shown have been omitted.

the same (100) sheet, make a dihedral angle of 9.3 (2)°, with an interplanar spacing of *ca* 3.52 Å and a ring-centroid separation of 3.711 (2) Å, However, there are no direction-specific intermolecular interactions between adjacent sheets.

Compound (V): In the structure of (V) (Fig. 1*b*) two C—H···π (arene) hydrogen bonds (Table 3), reinforced by a $\pi\cdots\pi$ stacking interaction between inversion-related pyridyl rings, link the molecules into sheets parallel to (100) (Fig. 4*a*). However, it is striking that the N73 atom in the pendent pyridyl does not act as a hydrogen-bond acceptor: the closest potential donor group, C3—H3 at $(x, y, -1+z)$, has C···N and H···N distances to N73 at (x, y, z) of 3.560 (3) and 2.65 Å, respectively, beyond the van der Waals sums.

Compound (XV): The aggregation in (XV) (Fig. 1*c*) differs significantly not only from that observed in (IV) and (V), but also from that found in (I), with which (XV) is formally isomorphous. The molecules are linked into complex sheets, using a total of five independent hydrogen bonds (Table 3), and it is convenient to regard a dimeric unit generated by paired C—H···N hydrogen bonds as the basic building block in the sheet formation. The aryl C72 atom in the molecule at (x, y, z) acts as a hydrogen-bond donor to the ring pyridyl N11 atom in the molecule at $(1-x, 1-y, 1-z)$, so generating by inversion an $R_2^2(14)$ (Bernstein *et al.*, 1995) dimer centred at (0.5, 0.5, 0.5). These dimers are linked into sheets by C—H···π hydrogen bonds involving both aryl and pyridyl rings as the acceptors, and a number of distinct motifs can be identified.

The aryl C103 atoms in the molecules at (x, y, z) and $(1-x, 1-y, 1-z)$, which lie in the dimer centred at (0.5, 0.5, 0.5), act as hydrogen-bond donors to the pendent pyridyl rings of the molecules at $(1-x, \frac{1}{2}+y, \frac{1}{2}-z)$ and $(x, \frac{1}{2}-y, \frac{1}{2}+z)$, respectively, and propagation of this interaction by the space group links the $R_2^2(14)$ dimer centred at (0.5, 0.5, 0.5) to four other dimers, centred at (0.5, 0, 0), (0.5, 1, 1), (0.5, 1, 0) and (0.5, 0, 1), so forming a sheet parallel to (100) (Fig. 4*b*). As in (IV) and (V) there is a single $\pi\cdots\pi$ stacking interaction within the sheet, again involving inversion-related pairs of fused pyridyl rings.

Although the 4-pyridyl compound (XV) is formally isomorphous with the phenyl compound (I), and although both compounds form hydrogen-bonded sheets parallel to (100), the hydrogen-bonded structure of (I) is much the simpler. Just two hydrogen bonds, one each of C—

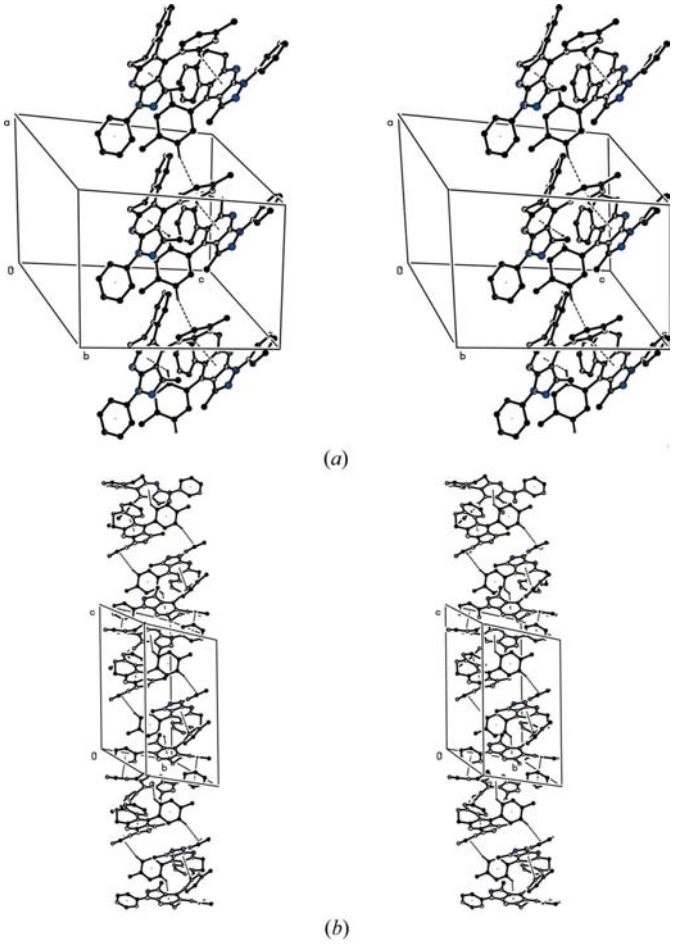

Figure 5
Stereoviews of parts of the crystal structure of (VIII) showing (*a*) the formation of a chain of rings along [100] built from two C—H···π(pyridyl) hydrogen bonds and one C—H···π(aryl) hydrogen bond; (*b*) the formation of a chain of rings along [001] built from two C—H···π(pyridyl) and two C—H···π(aryl) hydrogen bonds. For the sake of clarity the H atoms not involved in the motifs shown have been omitted.

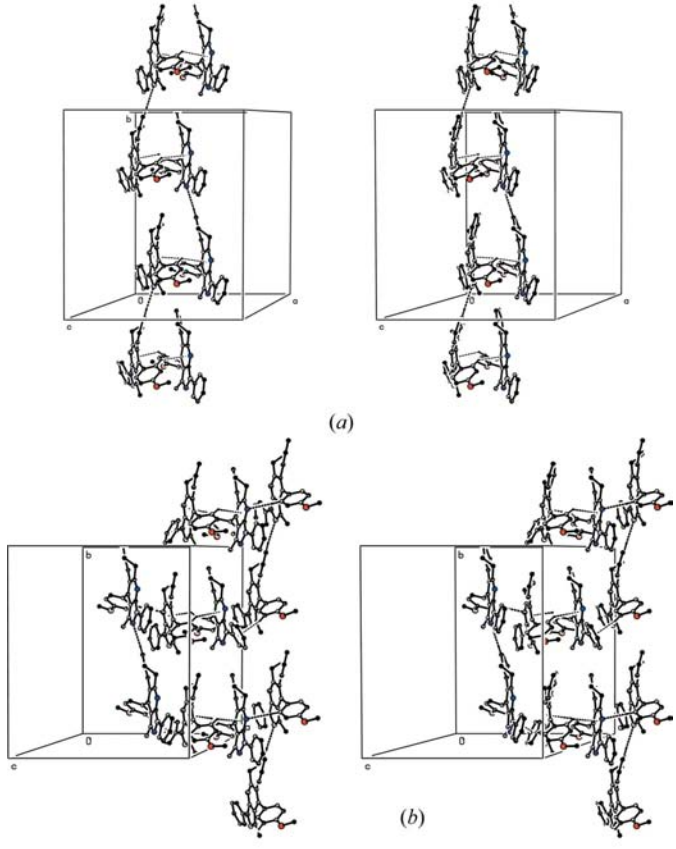

Figure 6
Stereoviews of parts of the crystal structure of (IX) showing (*a*) the formation of a chain of rings along (0.5, *y*, 0.75) built from only two of the four molecules; and (*b*) the formation of a chain along (1, *y*, 0.75) containing all four of the independent molecules. For the sake of clarity the H atoms not involved in the motifs shown have been omitted.

H···π(arene) and C—H···π(pyridyl) types, and propagated respectively by a glide plane and by an inversion centre, suffice to generate the sheet in (I), as opposed to the five interactions in (XV).

General comments on Series A: Although the 4-methylphenyl and 4-chlorophenyl compounds (II) and (IV), respectively, are isostructural, and the 4-pyridyl derivative (XV) is formally isomorphous with the phenyl compound (I), the 3-pyridyl derivative (V) is not isomorphous either with (I) or with (XV). All the structurally characterized compounds in series *A*, (I)–(V) and (XV) exhibit $\pi\cdots\pi$ stacking interactions. In the isomorphous pair (II) and (IV), this interaction involves pyridyl and fused phenyl rings in a pair of inversion-related molecules, but these rings are inclined to one another by 11.1 (2)° in (II) (Portilla *et al.*, 2005*b*) and 9.3 (2)° in (IV). By contrast, in each of (I), (III), (V) and (XV) the π-stacking interaction involves the fused pyridyl rings in a pair in inversion-related molecules, so that these rings are strictly parallel, with interplanar spacings ranging from 3.524 (2) Å in (V) to 3.849 (2) Å in (III) (Portilla *et al.*, 2005*b*). In (V) the ring-centroid offset is almost ideal at 1.593 (2) Å, but in each of (I), (II) and (XV) the offsets are very much less [0.461 (2), 0.655 (2) and 0.579 (2) Å respectively], indicative of stacking interactions which are likely to be repulsive rather than attractive (Hunter, 1994).

The hydrogen bonds in (I), (II), (IV) and (V) are all of C—H···π types, while the structures of (III) and (XV) both contain C—H···N hydrogen bonds, and that of (III) also contains a C—H···O hydrogen bond. The hydrogen-bonded structures of (I), (II), (IV), (V) and (XV) are all two-dimensional, whereas that of (III) is three-dimensional. However, it is possible to identify within the hydrogen-bonded structure of (II) a two-dimensional substructure built from C—H···N and C—H···π hydrogen bonds only. Throughout series *A*, the $\pi\cdots\pi$ stacking interactions, whether they involve parallel or non-parallel rings lie within the sheets built from the C—H···π and C—H···N hydrogen bonds

3.3.2. Series B. *Compound (VIII)*: The two independent molecules of (VIII) (Fig. 2) are linked into sheets by five C—H···π hydrogen bonds, but C—H···N hydrogen bonds are absent (Table 3). Within the selected asymmetric units the molecules are linked by two C—H···π(pyridyl) hydrogen bonds: aryl atoms H122 and H222 act as hydrogen-bond donors, respectively, to the pyridyl rings containing N27 and N17, to form a cyclic dimer having approximate twofold rotational symmetry. Dimeric units of this type are then linked by the C—H···π(arene) hydrogen bonds into sheets, whose formation is readily analysed in terms of two one-dimensional substructures.

In the first substructure the aryl C225 atom at (x, y, z) acts as a hydrogen-bond donor to the aryl ring (C121–C126) at $(-1+x, y, z)$, so linking the cyclic dimers into a chain of rings running parallel to the [100] direction (Fig. 5*a*). In the second substructure, atoms H21 and H125 at (x, y, z) act as donors, respectively, to the aryl rings (C281–C286) at $(1-x, 1-y, 2-z)$ and (C181–C186) at $(1-x, 1-y, 1-z)$, hence generating by inversion a chain of edge-fused rings running parallel to the [001] direction (Fig. 5*b*). The combination of the [100] and [001] chains generates a sheet parallel to (010), but there are no direction-specific interactions between adjacent sheets: in particular $\pi\cdots\pi$ stacking interactions are absent from the structure of (VIII).

Compound (IX): There are four independent molecules in (IX) (Fig. 3), and the asymmetric unit has been selected so that these molecules are linked by two C—H···N hydrogen bonds and two C—H···π (pyridyl) hydrogen bonds (Table 3). The resulting four-molecule aggregates are linked by three further hydrogen bonds, two of the C—H···π (pyridyl) type and one of the C—H···π (aryl) type, into sheets of some complexity, whose formation can be considered in terms of two simpler substructures. The first substructure involves only two of the four independent molecules: C222 and C322 atoms at (x, y, z) act as hydrogen-bond donors, respectively, to the pyridyl rings containing N37 at $(1-x, -\frac{1}{2}+y, \frac{3}{2}-z)$, and N27 at $(1-x, \frac{1}{2}+y, \frac{3}{2}-z)$, so forming a chain of edge-fused rings running parallel to the [010] direction, and generated by the 2_1 screw axis along $(\frac{1}{2}, y, \frac{3}{4})$ (Fig. 6*a*).

The second substructure involves all four molecules: the C225 atom at (x, y, z) acts as a hydrogen-bond donor to the aryl ring (C181–C186) at $(2-x, -\frac{1}{2}+y, \frac{3}{2}-z)$, so forming continuous chains parallel to [010] containing five different hydrogen bonds and generated by the 2~1~ screw axis along (1, y, 0.75) (see Fig. 6*b*). A combination of the two types of [010] chain generates a sheet parallel to (001). Two such sheets, which are generated by the screw axes at y = 0.25 and 0.75 and which are related to one another by inversion, pass through each unit cell, but there are no direction-specific interactions between adjacent sheets.

Compound (XIV): The molecules of (XIV) (Fig. 1*d*) are linked into simple chains by a single C—H···π(pyridyl) hydrogen bond (Table 3). The aryl C82 atom in the molecule at (x, y, z) acts as a hydrogen-bond donor to the pyridyl ring of the molecule at $(x, 1-y, -\frac{1}{2}+z)$, so forming a chain running parallel to the [001] direction and generated by the *c*-glide plane at y = 0.5 (Fig. 7). Two such chains, related to one another by translation, pass through each unit cell, but there are no direction-specific interactions between the chains.

General comments on Series B: In contrast to the isostructural pair in series *A*, (II) and (IV), the analogous compounds

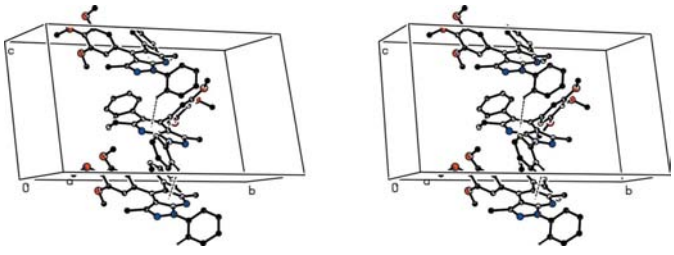

Figure 7
A stereoview of part of the crystal structure of (XIV) showing the formation of chains along [001] built from C—H···π(pyridyl) hydrogen bonds. For the sake of clarity the H atoms not involved in the motif shown have been omitted.

in series *B*, (VIII) reported here and (X) (Serrano *et al.*, 2005*a*), are not isostructural, even though both crystallize in the space group $P\bar{1}$, as they crystallize with Z' values of 2 and 1, respectively. Moreover, while the supramolecular structure of (VIII) is two-dimensional, that of (X) is only one-dimensional. In contrast to the structures in series *A*, where $\pi\cdots\pi$ stacking appears to be generally prevalent, there are no $\pi\cdots\pi$ stacking interactions in any of the structures in series *B* so far reported, either previously (Portilla, Serrano *et al.*, 2005; Serrano *et al.*, 2005*a*,*b*) or in this report. The isomeric pyridyl compounds in series *B*, (XI) and (XII), both adopt simple supramolecular structures (Portilla, Serrano *et al.*, 2005). The 3-pyridyl compound (XI) forms cyclic tetramers, formed by the propagation of a single C—H···N hydrogen bond by a $\bar{4}$ axis, while in the structure of the 4-pyridyl isomer (XII) there are no direction-specific intermolecular interactions of any kind.

4. Concluding discussion

We briefly compare here the structures of all the compounds in the two series *A* and *B*, concentrating in particular on two aspects: the structural effects of the pendent substituent (see Scheme 1), and comparisons within the strictly isomeric pairs in the two series.

Actions of the pendent aryl/pyridyl substituents: With the exceptions of (I), (II) and (VIII), all of the compounds in series *A* and *B* whose structures are now known carry pendent aryl or pyridyl substituents containing potential hydrogen-bond acceptor sites. However, it is surprising how infrequently these potential acceptors actually participate in the supramolecular aggregation.

Thus, of the three compounds (III), (IX) and (XIV) carrying methoxy substituents on the pendent aryl ring, the 4-methoxyphenyl derivative from series *A*, (III), is the only one in which the methoxy O atom acts as a hydrogen-bond acceptor (Portilla *et al.*, 2005*b*). In the compounds containing 4-halophenyl substituents, (IV) in series *A* and the isostructural compounds (X) and (XIII) in series *B*, there is no participation by the halogen substituents in either C—H···Cl or C—H···Br interactions: contacts of these types have been characterized (Brammer *et al.*, 2001) as lying at the outer limit of hydrogen-bonding behaviour, particularly the C—H···Br contacts, with correspondingly modest interaction energies, so that their absence from both series *A* and *B* is not unexpected.

It is the hydrogen-bonding behaviour of the pendent pyridyl rings in (V), (XI), (XII) and (XV) which is the least easy to rationalize or understand. Of the two pyridyl derivatives reported here from series *A*, the structure of the 3-pyridyl compound (V) contains no C—H···N hydrogen bonds, while the 4-pyridyl derivative (XV) exhibits one hydrogen bond of this type, but having one of the fused-ring N atoms as the acceptor. Thus, in neither of these compounds does the N atom of the pendent pyridyl ring participate in the hydrogen bonding, despite the expectation that such N atoms should be strongly basic acceptors at sites which are sterically unhindered, However, the pendent pyridyl ring acts as an acceptor in a C—H···π(pyridyl) hydrogen bond in (XV), although not in (V): this apparent preference for a C—H···π hydrogen bond over a C—H···N hydrogen bond is unexpected. The isomeric compounds (XI) and (XII) from series *B* showed markedly different hydrogen-bonding behaviour (Portilla, Serrano *et al.*, 2005). In (XI) the N atom of the pendent 3-pyridyl substituent acts as the acceptor in a C—H···N hydrogen bond, in the only such example in these two series, but in the structure of the 4-pyridyl isomer there are no direction-specific interactions of any kind between the molecules. In particular, the N atom of the pendent 4-pyridyl unit does not act as a hydrogen-bond acceptor, nor do these pendent rings in (XI) and (XII) act as acceptors in C—H···π(pyridyl) hydrogen bonds.

Comparison of the isomeric pairs in Series A and B: Here we briefly compare the crystal structures of the isomeric pairs of compounds, one from each of series *A* and *B*, namely (II) and (VIII), (II) and (IX), (IV) and (X), and (V) and (XI), and in addition, we compare (XV) and (XII). It is unfortunate that we have not been able to compare the structures of the parent isomers, (I) and (VII).

The isomers (II) and (VIII) crystallize in different crystal systems with different values of Z', 1 in (II) and 2 in (VIII). Despite this, both isomers form two-dimensional structures built solely from C—H···π hydrogen bonds: while (II) utilizes only aryl rings as hydrogen-bond acceptors, (VIII) utilizes both aryl and pyridyl rings as the acceptors. While (II) and (IV) in series *A* are isostructural, their isomers in series *B*, (VIII) and (X), are not isostructural. Isomers (IV) and (X) both crystallize with $Z' = 1$, and the supramolecular aggregation in both compounds depends solely on two independent C—H···π(arene) hydrogen bonds: however, the resulting hydrogen-bonded structures are two-dimensional in (IV), but only one-dimensional in (X). The isomers (II) and (IX) crystallize with Z' values of 1 and 4, respectively, and the structures of both isomers exhibit a range of different hydrogen bonds, leading to structures which are three-dimensional in (III) and two-dimensional in (IX). Surprisingly, the $Z' = 1$ structure (III) is of higher dimensionality than the $Z' = 4$ structure (IX).

The pair of isomers (V) and (XI) provides perhaps the most striking contrast within these isomer series. Firstly, they crystallize in markedly different space groups [$P2_1/c$ for (V) and $P\bar{4}2_1c$ for (XI), albeit with $Z' = 1$ in each case]; secondly, while the supramolecular aggregation in (V) is controlled by two independent C—H···π(arene) hydrogen bonds, that in (XI) depends upon a single C—H···N hydrogen bond; and thirdly, while the molecules of (V) are linked into sheets, those of (XI) form cyclic tetramers, so that the supramolecular aggregation of (XI) is finite and it can thus be regarded as zero-dimensional.

Similar divergences of behaviour are observed within the pair (XV) and (XII), although these are not strictly isomeric; however, (XV) is isomorphous with (I). Again, this pair of compounds crystallize with markedly different space groups, $P2_1/c$ with $Z' = 1$ for (XV) and $P2_12_12_1$ with $Z' = 2$ for (XII); in (XV) there are intermolecular hydrogen bonds of C—H···N,

C—H···π(arene) and C—H···π(pyridyl) types leading to a complex two-dimensional structure, whereas in (XII) there are no direction-specific intermolecular interactions of any kind, so the structure of (XII) consists of effectively isolated molecules.

There are thus marked differences, both in the nature of the direction-specific intermolecular interactions and in the resulting crystal structures, which arise from quite modest changes in the pendent aryl or pyridyl substituent where, as noted above, this substituent rarely plays a direct role in the aggregation, or from the orientation of the terminal aryl ring of the fused ring system. Such structural variations arising from simple changes in molecular constitution present a keen test for computational attempts at the *ab initio* prediction of the crystal structures of molecular compounds, an endeavour where convincing success remains tantalisingly elusive (Lommerse *et al.*, 2000; Motherwell *et al.*, 2002; Day *et al.*, 2005).

X-ray data were collected at the EPSRC X-ray Crystallographic Service, University of Southampton. MN, JMT and JC thank the Consejería de Innovación, Ciencia y Empresa (Junta de Andalucía, Spain) and the Universidad de Jaén for financial support, including a scholarship grant to JMT. JP and JQ thank COLCIENCIAS and UNIVALLE (Universidad del Valle, Colombia) for financial support.

References

Bernstein, J., Davis, R., Shimoni, L. & Chang, N.-L. (1995). *Angew. Chem. Int. Ed. Engl.* **34**, 1555–1573.
Brammer, L., Bruton, E. A. & Sherwood, P. (2001). *Cryst. Growth Des.* **1**, 277–290.
Burla, M. C., Caliandro, R., Camalli, M., Carrozzini, B., Cascarano, G. L., De Caro, L., Giacovazzo, C., Polidori, G. & Spagna, R. (2005). *J. Appl. Cryst.* **38**, 381–388.
Cremer, D. & Pople, J. A. (1975). *J. Am. Chem. Soc.* **97**, 1354–1358.
Day, G. M. *et al.* (2005). *Acta Cryst.* B**61**, 511–527.
Ferguson, G. (1999). *PRPKAPPA*. University of Guelph, Canada.
Hooft, R. W. W. (1999). *COLLECT*. Nonius BV, Delft, The Netherlands.
Hunter, C. A. (1994). *Chem. Soc. Rev.* **23**, 101–109.
Lommerse, J. P. M. *et al.* (2000). *Acta Cryst.* B**56**, 697–714.
McArdle, P. (2003). *OSCAIL for Windows*, Version 10. Crystallography Centre, Chemistry Department, NUI Galway, Ireland.
Motherwell, W. D. S. *et al.* (2002). *Acta Cryst.* B**58**, 647–661.
Naylor, R. E. & Wilson, E. B. (1957). *J. Chem. Phys.* **26**, 1057–1060.
Nishio, M. (2004). *CrystEngComm*, **6**, 130–158.
Otwinowski, Z. & Minor, W. (1997). *Methods in Enzymology*, Vol. 276, *Macromolecular Crystallography*, edited by C. W. Carter Jr & R. M. Sweet, Part A, pp. 307–326. New York: Academic Press.
Portilla, J., Quiroga, J., Cobo, J., Low, J. N. & Glidewell, C. (2005*a*). *Acta Cryst.* C**61**, o452–o456.
Portilla, J., Quiroga, J., Cobo, J., Low, J. N. & Glidewell, C. (2005*b*). *Acta Cryst.* C**61**, o483–o489.
Portilla, J., Serrano, H., Cobo, J., Low, J. N. & Glidewell, C. (2005). *Acta Cryst.* C**61**, o490–o492.
Quiroga, J., Mejía, D., Insuasty, B., Abonía, R., Nogueras, M., Sánchez, A., Cobo, J. & Low, J. N. (2001). *Tetrahedron*, **57**, 6947–6953.
Riddell, F. & Rogerson, M. (1996). *J. Chem. Soc. Perkin Trans. 2*, pp. 493–504.
Riddell, F. & Rogerson, M. (1997). *J. Chem. Soc. Perkin Trans. 2*, pp. 249–255.
Serrano, H., Quiroga, J., Cobo, J., Low, J. N. & Glidewell, C. (2005*a*). *Acta Cryst.* E**61**, o1058–o1060.
Serrano, H., Quiroga, J., Cobo, J., Low, J. N. & Glidewell, C. (2005*b*). *Acta Cryst.* E**61**, o1702–o1703.
Sheldrick, G. M. (2003). *SADABS*, Version 2.10. University of Göttingen, Germany.
Sheldrick, G. M. (2008). *Acta Cryst.* A**64**, 112–122.
Spek, A. L. (2003). *J. Appl. Cryst.* **36**, 7–13.
Tannenbaum, E., Myers, R. J. & Gwinn, W. D. (1956). *J. Chem. Phys.* **25**, 42–47.
Wilson, A. J. C. (1976). *Acta Cryst.* A**32**, 994–996.